Liquid Crystals
Publication details, including instructions for authors and subscription information:
http://www.informaworld.com/smpp/title~content=t713926090

Influence of the proximity of a N*-SmA-SmC* multicritical point on the electroclinic effect in the cholesteric phase

J. Hemine[a]; C. Legrand[b]; A. Daoudi[c]; N. Isaert[d]; H. T. Nguyen[e]
[a] Laboratoire de Physique de la Matière Condensée, Université Hassan II, Mohammedia, Morocco [b] Laboratoire d'Etude des Matériaux et des Composants pour l'Electronique, E.A. 2601, Université du Littoral-Côte d'Opale B.P. 717, Calais, France [c] Laboratoire de Thermophysique de la Matière Condensée (Equipe de l'UMR CNRS n°8024), Université du Littoral-Côte d'Opale, 145, 59 140 Dunkerque, France [d] Laboratoire de Dynamique et Structures des Matériaux Moléculaires, UMR CNRS n°8024, Université de Lille 1, 59655 Villeneuve d'Ascq, France [e] Centre de Recherche Paul Pascal, Université de Bordeaux 1, 33600 Pessac, France

To cite this Article Hemine, J. , Legrand, C. , Daoudi, A. , Isaert, N. and Nguyen, H. T.(2007) 'Influence of the proximity of a N*-SmA-SmC* multicritical point on the electroclinic effect in the cholesteric phase', Liquid Crystals, 34: 2, 241 — 249
To link to this Article: DOI: 10.1080/02678290601097326
URL: http://dx.doi.org/10.1080/02678290601097326

Liquid Crystals, Vol. 34, No. 2, February 2007, 241–249

Influence of the proximity of a N*–SmA–SmC* multicritical point on the electroclinic effect in the cholesteric phase

J. HEMINE*†, C. LEGRAND‡, A. DAOUDI§, N. ISAERT* and H. T. NGUYEN¶

†Laboratoire de Physique de la Matière Condensée, Université Hassan II, F.S.T. Mohammedia B.P. 146, Mohammedia, Morocco

‡Laboratoire d'Etude des Matériaux et des Composants pour l'Electronique, E.A. 2601, Université du Littoral-Côte d'Opale B.P. 717, Calais, France

§Laboratoire de Thermophysique de la Matière Condensée (Equipe de l'UMR CNRS n°8024), Université du Littoral-Côte d'Opale, 145, Avenue Maurice Schumann, 59 140 Dunkerque, France

*Laboratoire de Dynamique et Structures des Matériaux Moléculaires, UMR CNRS n°8024, Université de Lille 1, 59655 Villeneuve d'Ascq, France

¶Centre de Recherche Paul Pascal, Université de Bordeaux 1, 33600 Pessac, France

(*Received 14 June 2006; accepted 23 October 2006*)

Chiral liquid crystal material (C12 homologue of biphenyl benzoate series) exhibiting the cholesteric (N*), smectic A (SmA) and ferroelectric smectic C (SmC*) phases have been studied by structural, thermodynamic, electrooptical and dielectric investigations. The helical pitch, tilt angle and spontaneous polarization have been determined. In the dielectric measurements, we have studied the soft mode in the SmC* and SmA phases. From experimental data, we have evaluated the soft-mode rotational viscosity and the electroclinic coefficient in the SmA phase. All results are discussed and compared with previous studies performed on other homologues of the same series. The main result is that the relaxation process detected in the N* phase for the C8, C10 and C11 homologues and explained as a soft-mode-like mechanism, is not observed for C12. This corroborates the idea that this mechanism is related to the appearance of smectic order fluctuations within N* phase, the amplitude of which is increased when approaching the SmC*–SmA–N* multicritical point.

1. Introduction

Over the last few decades, there has been considerable interest in experimental and theoretical studies carried out to understand the electroclinic effect near to a SmC*–SmA phase transition [1, 2]. This effect corresponds to an induced tilt angle of molecules when an electric field is applied parallel to the smectic plane. It is well known that for low applied electric field, the induced tilt in the SmA phase is proportional to the amplitude of the applied electric field. The coefficient of this proportionality is thus the electroclinic coefficient, e_C, which is related to the induced polarization, P_{ind}, in the SmA phase. At a given amplitude of the electric field, the induced tilt is higher near to the SmC*–SmA phase transition, whereas the switching time is lower far below this phase transition. If the compounds show high values of the spontaneous polarization in the SmC* phase, the induced polarization in the SmA phase can grow to very high values. Therefore, for materials of the biphenyl alkyloxy benzoates series [3], which have a very high polarization, the amplitude of the electroclinic effect is much more important near the SmC*–SmA and SmA–N* phase transitions, especially in the vicinity of the SmC*–SmA–N* multicritical point [3]. The discovery of materials exhibiting the N*–SmA–SmC* phase transition has attracted the attention of many authors [4, 5]. The principal reason is that the electroclinic effect observed and reported in the SmA and SmC* phases, can be again detected and measured optically [6, 7] and dielectrically [8, 9] in the N* phase. Meyer's theory of the electroclinic effect in the N* phase and its prediction near an N*AC* multicritical point have been extended by Marcerou [10]. He has shown that the trilinear coupling between the smectic layers, the tilt angle and the electric polarization is responsible for the electroclinic effect in the SmC*, SmA and N* phases, especially in the proximity of an N*AC* multicritical point. In a previous paper, we have detected at high frequencies, a relaxation process in the N* phase for the C8, C10 and C11 [11] substances (see table 1). We have interpreted this relaxation

*Corresponding author. Email: hminefr@yahoo.fr

Liquid Crystals
ISSN 0267-8292 print/ISSN 1366-5855 online © 2007 Taylor & Francis
http://www.tandf.co.uk/journals
DOI: 10.1080/02678290601097326

Table 1. Chemical formula, phase sequences and transition temperatures (°C) for the homologues of the biphenyl benzoate series. The abbreviations used in this table are: Cr: crystalline phase; Sm: smectic phases A, C*; N*: cholesteric phase; BP: blue phase; I: isotropic phase; •: the phase exists; –: the phase does not exist; ( ): monotropic transition.

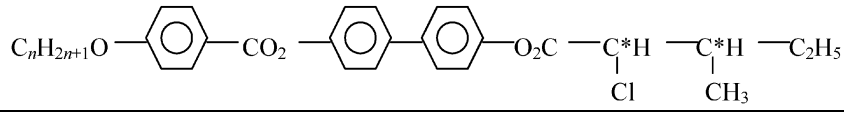

n	Cr		Sm		SmC*		SmA		N*		BP		I
7	•	100	•	(52)	•	134	–		•	166	•	166.1	•
8	•	88	–		•	138	–		•	165.5	•	166.5	•
9	•	89	–		•	142	–		•	162	•	162.1	•
10	•	88	–		•	143	•	144	•	159	•	160	•
11	•	88	–		•	146	•	149	•	157	•	157.1	•
12	•	81	–		•	145.5	•	150	•	154	•	154.5	•

mechanism as an electroclinic effect which has a relatively high amplitude in the proximity of an N*–SmA–SmC* multicritical point.

In this paper, we will discuss how the dielectric relaxation process, observed in the N* phase for C8, C10 and C11 homologues, disappears for C12 compound. For this purpose, we have performed a complete experimental characterization of C12, including structural, thermodynamic, electrooptical as well as dielectric investigations. We have measured the helical pitch as a function of temperature in the SmC* and N* phases. The temperature dependences of the tilt angle and spontaneous polarization of the SmC* phase have been studied. We also report in this work the thermodynamic behaviour under pressure of C12 in order to study the stability of smectic and cholesteric phases involved in the N*–SmA–SmC* phase sequence. Using the dielectric spectroscopy method, we have investigated the relaxation mechanisms related to ferroelectricity or/and smectic orders. The relaxation frequencies and dielectric strengths of these mechanisms are measured as a function of temperature near to the SmC*–SmA and SmA–N* transition temperatures.

2. Experimental

Six pure compounds of the homologous biphenyl alkyloxy benzoate series, exhibiting the SmC*–SmA, SmA–N*, SmC*–N* and N*–BP phase transitions, have been synthesized [3]. The chemical structure, phase sequences and transition temperatures at atmospheric pressure determined both by polarized optical microscopy and differential scanning calorimetry are summarized in table 1. It can be seen from table 1 that the first three compounds of the series (from C7 to C9) do not exhibit the SmA phase. The temperature range of the SmA phase increases from 1, 3 to 4.5°C for C10, C11 and C12, respectively. The N*–SmA–SmC* multicritical point is approached as the length of the alkyloxy chain is decreased. For this reason, we focused our experimental studies on C12 compound, for which we suspected that the relaxation process observed near a multicritical point for C8, C10 and C11 derivatives, disappears completely for C12 far from this multicritical point.

The helical pitch was measured by the Grandjean–Cano method [12, 13] with prismatic planar samples in the N* phase, and prismatic pseudo-homeotropic samples in the SmC* phase. In the N* phase, the molecules are parallel to the glass surfaces and the helical axis is perpendicular to the sample plane. For SmC* phase, pseudo-homeotropic samples were prepared, which lead to an orientation of the helical axis of the SmC* structure perpendicular to the glass plates.

The spontaneous polarization, P_s, and tilt angle, θ, were measured as a function of temperature. For these studies, a surface stabilized cells [14] with polyvinyl alcohol (PVA) aligning layers were used to promote a planar alignment of molecules. The thickness of the cells is about 3 µm. The tilt angle measurements were performed in the linear regime of the light detection between crossed polarizers by applying a 0.2 Hz square wave voltage at $5\,V\,\mu m^{-1}$ electric field amplitude to samples. To measure P_s, a 1 kHz triangular wave of $5\,V\,\mu m^{-1}$ amplitude was applied to the cells.

The pressure effect on the phase behaviour was carried out by thermobarometric analysis (TBA). This method consists of recording the pressure variation versus temperature of a sample (about 10 mg) at constant volume. A heating rate of $2^{\circ}C\,min^{-1}$ was used for the thermobarometric measurements. The complete TBA description and set up have been extensively discussed in previous papers [15].

The measurements of the complex permittivity were carried out in the frequency range 5 Hz to 1 MHz on planar samples, with smectic layers perpendicular to the electrodes (bookshelf geometry) using a previously

described experimental procedure [16]. To obtain a good alignment, the sample was introduced in the cell by capillarity in the isotropic phase. The cell thickness of 30 µm, was chosen much higher than the helical pitch value (≈2 µm) to obtain a planar winding state in the SmC* phase. To check the sample alignment and transition temperatures, the samples were observed by means of a polarizing microscope in reflection mode. The electric field was applied normal to the helical axis of the SmC* structure and parallel to the smectic layers. The measurements were made in two steps: with and without superimposition of a dc bias field to measuring ac voltage. The complex permittivity, $\varepsilon^*(f, T)$, for the distribution of the Cole–Cole type may be written as:

$$\varepsilon^* - \varepsilon(\infty) = \frac{\Delta\varepsilon_G}{1+(jf/f_G)^{1-\alpha_G}} + \frac{\Delta\varepsilon_S}{1+(jf/f_S)^{1-\alpha_S}} \quad (1)$$

where $\varepsilon(\infty)$ represents the limit of the dielectric permittivity at high frequencies range and f_i, α_i and $\Delta\varepsilon_i$ are the relaxation frequency, the corresponding distribution parameter and the dielectric strength, respectively, of the relaxation mode i.

3. Results

3.1. *Helical pitch measurements*

To measure the helical pitch, we obtained excellent planar and pseudo-homeotropic orientations of the samples, which allowed the observation of regular steps (Grandjean–Cano lines) in the N* and SmC* phases. Figure 1 shows the temperature dependence of the helical pitch in the N* and SmC* phases. In the N* phase, the helical pitch is very short ($p\sim0.25$ µm) near the N*–BP transition temperature, and sligthly increases when going towards the N*–SmA transition temperature. It then rapidly increases and diverges at the N*–SmA transition. In the SmC* phase, we have

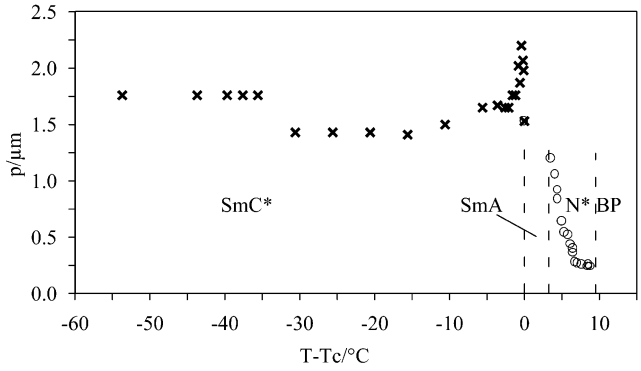

Figure 1. Helical pitch versus temperature in the SmC* (**x**) and N* (○) phases for C12.

obtained two temperature ranges where the helical pitch is constant: $p\sim1.75$ µm in the temperature range $35.6 \leqslant T_C - T \leqslant 53.7$°C, and p~1.4 µm for $15.6 \leqslant T_C - T \leqslant 30.6$°C, where T_C is the SmC*–SmA transition temperature. When approaching the SmA phase, the pitch increases up to 2.2 µm. Close to T_C, the Grandjean–Cano lines may become invisible because the rotator power cancels with the tilt angle. The pseudo-homeotropic 'flat drop' method [17] has been used and gives the limit value of $p\sim1.5$ µm at T_C.

3.2. *Electrooptical properties*

Figure 2 gives the temperature dependence of the tilt angle and the spontaneous polarization of the C12 material. At low temperatures and far from T_C, a tilt angle of 35° was measured. With increasing temperature, θ rapidly decreases when approaching T_C. As can be seen from figure 2, this compound presents a high spontaneous polarization of about 140 nC cm^{-2} at low temperatures. The high value of P_s obtained for this compound is principally due to the presence of the ester group –COO–, which links the chiral alkyloxy chain to

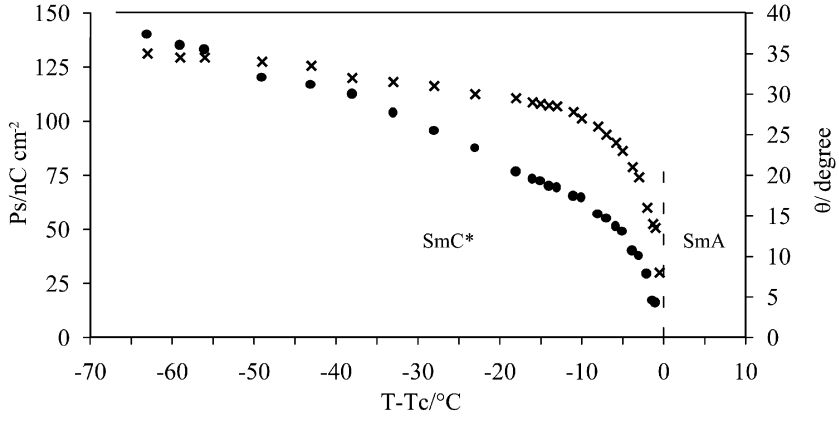

Figure 2. Tilt angle θ (**x**) and spontaneous polarization P_s (●) versus temperature for C12.

the biphenyl core, near to an electron-attracting Cl atom. For homologues with shorter alkyloxy chains, values of P_S=200 and 160 nC cm^{-2} have already been reported for C8 and C11, respectively [3, 11]. Therefore, for this series of homologues, decreasing the alkyloxy chain length results in an increase of the ferroelectric polarization. This effect can be merely understood by the fact that for the C12 compound, the longer alkyloxy chain hinders a rotational motion of the molecules [4] compared to C8 and C11, leading to a decrease of the amplitude of the spontaneous polarization.

3.3. *Dielectric responses*

3.3.1. Dielectric measurements without a dc bias. For the C12 compound, the dielectric spectra in the SmA phase display one relaxation mechanism at higher frequencies. The dielectric strength of this mechanism increases as the temperature T_C is approached from the SmA phase. That is why this mechanism was attributed to the soft mode.

The temperature dependence of the dielectric strength, $\Delta\varepsilon_S$, and the relaxation frequency, f_S, of the soft-mode in the SmA phase are depicted in figures 3 and 4, respectively. The reciprocal dielectric strength, $\Delta\varepsilon_S{}^{-1}$, and f_S linearly depend on T–T_C (see figures 3 and 4). Such behaviour agrees with the theoretical model [18], which predicts that $\Delta\varepsilon_S$ and f_S satisfy the Curie–Weiss law close **to** T_C. The values of $\Delta\varepsilon_S$ and f_S vary from 0.7 and 324 kHz far from T_C to 15 and 25 kHz at $T=T_C$, respectively (these values are higher than those measured for C10 material [3]). However, unlike the C8, C10 and C11 homologues [3, 11], we do not observe in the N* phase of C12 any relaxation mechanism in the high frequency range.

3.3.2. Dielectric measurements with a dc bias. To observe the soft-mode in the SmC* phase, a dc bias field of 1 V μm^{-1} was superimposed to the measuring ac voltage. This value is sufficiently high to unwind the helical structure in the SmC* phase. This leads to a

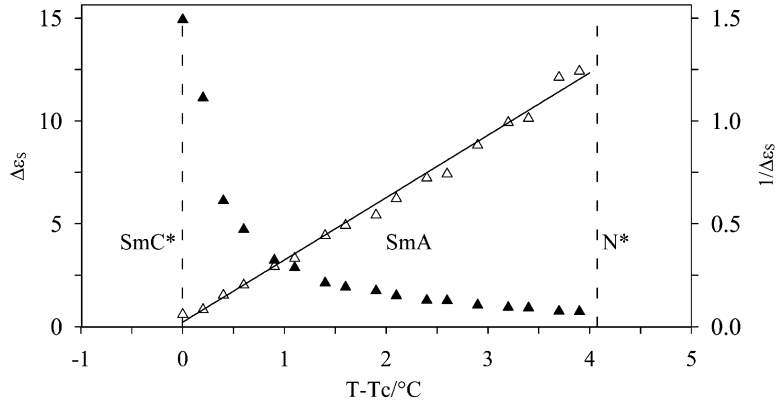

Figure 3. Dielectric strength (▲) and reciprocal dielectric strength (△) of the soft-mode in the SmA phase versus temperature for C12. Measurements were made without a dc bias.

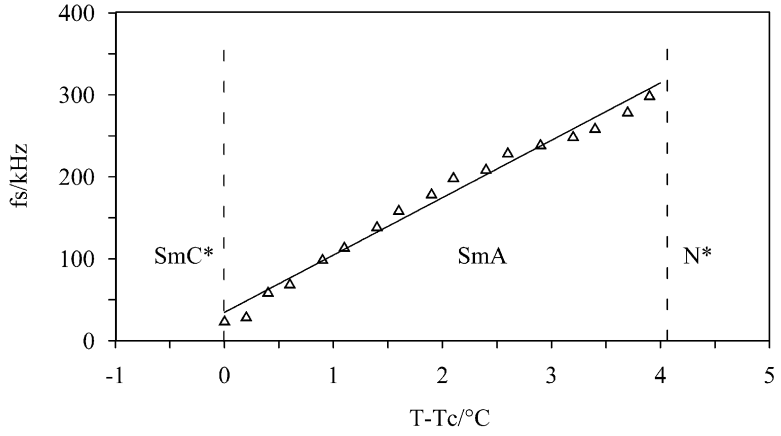

Figure 4. Relaxation frequency of the soft-mode versus temperature in the SmA phase for C12. Measurements were made without a dc bias.

spatially homogeneous structure; the Goldstone-mode was then suppressed and the soft-mode can be observed in SmC* phase. The temperature dependence of the dielectric strength and of the relaxation frequency obtained for C12 under a bias field is reported in figures 5 and 6, respectively. In the SmC* phase and far from T_C, the dielectric strength is small ($\Delta\varepsilon_S \sim 0.5$), and then continuously increases with temperature between $T_C - T = 1.7$ and 0.7°C. When approaching T_C, $\Delta\varepsilon_S$ rapidly increases and reaches its maximum value of $\Delta\varepsilon_S = 5.24$ at T_C. A similar behaviour of $\Delta\varepsilon_S$ is obtained in the SmA phase (figure 5) when the temperature decreases. We can also notice that, far from T_C and near the SmA–N* transition, we obtained in the SmA phase the same value of $\Delta\varepsilon_S$ (~0.5) than that obtained without bias field. Furthermore, ${\Delta\varepsilon_S}^{-1}$ and f_S in the SmC* and SmA phases are linearly dependent on temperature (see figures 5 and 6). This qualitative behaviour agrees with the theoretical model [18], and was already observed and studied by other authors [16, 19]. Far from T_C, f_S in the SmA phase (~460 kHz) is two times higher than that obtained in the SmC* phase (~220 kHz). It is instructive to compare the experimental values of $\Delta\varepsilon_S$ and f_S measured here at T_C for C12 with those obtained for C10 [3] under a 1 Vμm^{-1} dc bias field. These values are gathered in table 2.

We can see from table 2 that $\Delta\varepsilon_S$ has the same order of magnitude at T_C both for C10 and C12 compounds, whereas the value of f_S for C12 is approximately 1.4 times larger than that obtained for C10. As has been previously observed for other homologues of the series [3], $\Delta\varepsilon_S$ and f_S at T_C are dependent on the dc bias field; $\Delta\varepsilon_S$ decreases and f_S is shifted to higher frequencies when a bias field is applied. These changes on $\Delta\varepsilon_S$ and f_S are due to the electroclinic effect, and enhanced by the relatively high value of the bias voltage. This high voltage is necessary to unwind the helical structure because of the low value of the pitch ($p \sim 2\,\mu$m near T_C)

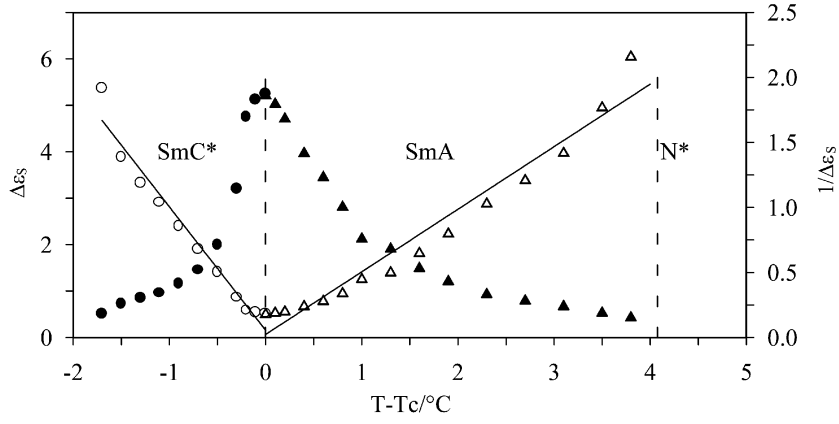

Figure 5. Dielectric strength (full symbols) and reciprocal dielectric strength (open symbols) of the soft-mode in the SmC* and SmA phases versus temperature for C12. Measurements were made with a dc bias field of $E = 1\,\mathrm{V}\,\mu\mathrm{m}^{-1}$.

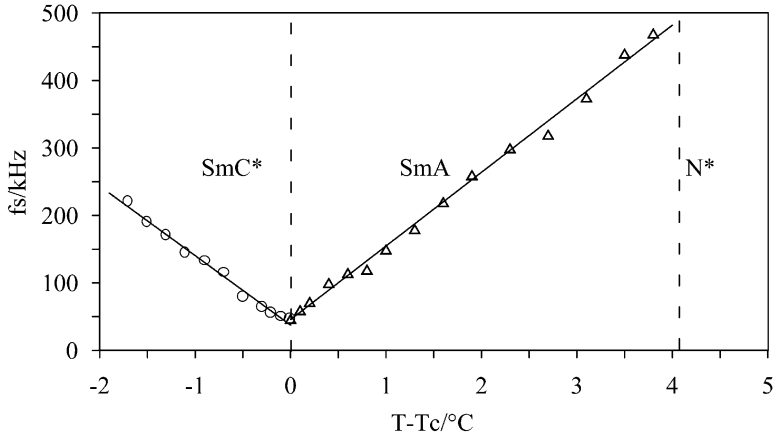

Figure 6. Relaxation frequency versus temperature of the soft-mode in the SmC* and SmA phases for C12. Measurements were made with a dc bias field of $E = 1\,\mathrm{V}\,\mu\mathrm{m}^{-1}$.

Table 2. Experimental values of $\Delta\varepsilon_S$ and f_S corresponding to the soft-mode mechanism for C10 and C12 at T_C.

Compound	$\Delta\varepsilon_S$	f_S (kHz)
C10	5	35
C12	5.25	50

in the SmC* phase. Unlike C8, C10 and C11 (see figure 7) homologues [3, 11] the dielectric response of the N* phase under bias field for C12 does not reveal any relaxation process at high frequencies.

4. Discussion

From structural, electrooptical and dielectric data, and using the predictions of the generalized Landau models [18], we can determine some characteristic parameters of the soft mode in the SmC* and SmA phases for the C12 homologue. The dielectric strength and the relaxation frequency of the soft mode in the SmA phase are given by:

$$\varepsilon_0\Delta\varepsilon_{SA} = \frac{(\chi C)^2}{K_{33}q^2 + \alpha(T - T_C)} \tag{2}$$

$$f_{SA} = \frac{K_{33}q^2 + \alpha(T - T_C)}{2\pi\gamma_{SA}} \tag{3}$$

where α is the usual coefficient contained in the temperature term of the Landau free-energy density expansion, $q=2\pi/p$ is the wave vector of the modulated SmC* phase, K_{33} is the twist elastic constant, χ and ε_0 are the generalized dielectric susceptibility and the permittivity of free space, respectively; C is the temperature independent coefficient of the piezoelectric bilinear coupling, and γ_{SA} is the rotational viscosity of the soft mode in the SmA phase. As we can see from equations (2)–(3), the reciprocal dielectric strength $1/(\varepsilon_0\Delta\varepsilon_{SA}) \cong \alpha(T-T_C)/\chi^2C^2$, and the relaxation frequency $f_{SA} \cong \alpha(T-T_C)/2\pi\gamma_{SA}$ of the soft mode in the SmA phase linearly decrease with temperature when approaching T_C. The elastic term, $(K_{33}q^2)$, was reasonably neglected

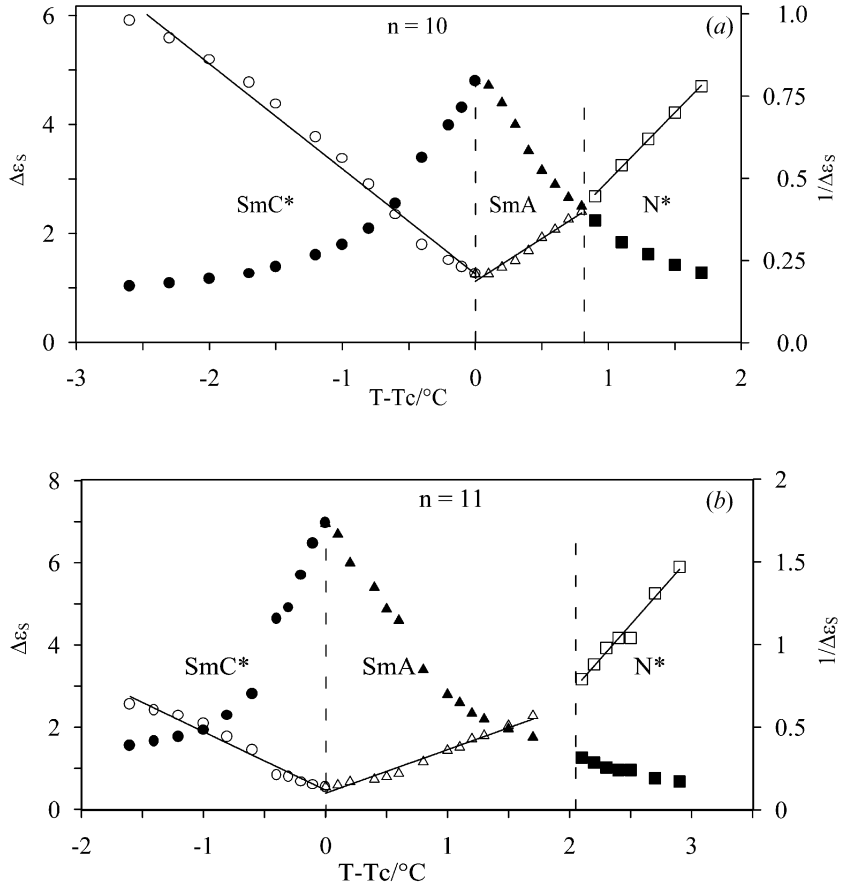

Figure 7. Dielectric strength (full symbols) and reciprocal dielectric strength (open symbols) of the soft-mode in the SmC* and SmA phases, and of the relaxation process observed in the N* phase versus temperature for C10 (a) and C11 (b) under a dc bias field of $E=1\,\mathrm{V\,\mu m^{-1}}$ [11].

here because the dielectric response of our system close to T_C is principally governed by the thermal term, $\alpha(T-T_C)$, which strongly influences the temperature dependence of $\Delta\varepsilon_{SA}$ and f_{SA} quantities. The experimental value of γ_{SA} can be calculated if the piezoelectric coefficient χC is known. We have estimated this coefficient near T_C, via the experimental data of P_S and θ. These characteristic parameters are related to each other as follows:

$$P_S \cong (\chi C)\theta. \tag{4}$$

From equations (2)–(4), we can write:

$$\gamma_{S_A} = \frac{\left(P_s/\theta\right)^2}{2\pi\varepsilon_0} \frac{\left(\mathrm{d}\Delta\varepsilon_s^{-1}/\mathrm{d}T\right)}{\left(\mathrm{d}f_s/\mathrm{d}T\right)}. \tag{5}$$

From the experimental data of figures 2–4 we found $P_s/\theta \cong \chi C = 0.7\,\mathrm{Cm}^{-2}$ and $\left(\mathrm{d}\Delta\varepsilon_s^{-1}/\mathrm{d}T\right)/(\mathrm{d}f_s/\mathrm{d}T) = 4.16\times10^{-3}\,\mathrm{kHz}^{-1}$. The estimated value of γ_{SA}, determined close to T_C, is found to be $\gamma_{SA}=37\,\mathrm{mPa\,s}$. From the data of figure 4, and using equation (3), we can also evaluate the α coefficient; we thus obtained $\alpha = 5.7\times10^4\,\mathrm{N\,m^{-2}\,K^{-1}}$. This value is comparable with that we have obtained for the C10 homologue [3], and with values reported for other compounds exhibiting the SmC*–SmA phase transition [20].

We shall now determine the soft mode relaxation time, $\tau_S = 1/2\pi f_S$, and the electroclinic coefficient, e_C, in the SmA phase close to T_C. From the Landau free-energy expansion, the temperature dependence of e_C is expressed as [18]:

$$e_C = \frac{\Delta\varepsilon_{SA}}{4\pi\chi C} = \frac{\chi \mathrm{C}}{\alpha(T-T_C)+K_{33}\,q^2}. \tag{6}$$

For the same reason mentioned above, we neglect in equation (6) the elastic term, $K_{33}q^2$, with respect to the thermal term $\alpha(T-T_C)$ ($\gg K_{33}q^2$). Figure 8 gives the temperature dependence of τ_S and e_C in the SmA phase for C12. As we can see, τ_S increases with decreasing temperature, and is found to vary from 6.5 µs at T_C to 0.5 µs when approaching the N* phase. The temperature dependence of e_C is characterized by a rapid decrease near T_C when T increases, followed by a slow decrease when going towards N* phase: e_C vary from $\sim 8^\circ\,\mu\mathrm{m\,V^{-1}}$ at T_C and decreases to $\sim 0.5^\circ\,\mu\mathrm{m\,V^{-1}}$ near the SmA–N* transition.

This experimental value of e_C in the SmA phase at $T \cong T_C$ is similar to that obtained for C10 [3]. Its value near the SmA–N* transition is however four times lower than that determined for C10. The values of e_C obtained for our compounds are much larger than those found by Li *et al.* [21], but are comparable with the results obtained by Bahr and Heppke [22] for ferroelectric liquid crystal materials with high spontaneous polarization. Bahr and Heppke found an e_C of about $5.7^\circ\,\mu\mathrm{m\,V^{-1}}$ at T_C, and $0.3^\circ\,\mu\mathrm{m\,V^{-1}}$ in the SmA phase far from T_C, values which agree with our results. The magnitude of the electroclinic coefficient is proportional to the piezoelectric coupling term χC, equation (6), which is related to the spontaneous polarization, equation (4), in the SmC* phase. Therefore, for our material which has a high polarization ($140\,\mathrm{nC\,cm^{-2}}$), the amplitude of e_C is much more important in the SmA phase, especially near the SmC*–SmA and SmA–N* phase transitions.

In our early studies [3], carried out on C10 compound, we have demonstrated that the relaxation process observed in the N* phase at high frequencies (~400 kHz), has the same behaviour as the soft-mode classically observed in the SmA phase. We have explained this effect as a soft mode caused by local fluctuations of smectic order [9], namely cybotactic groups, within N* phase [6]. These fluctuations are

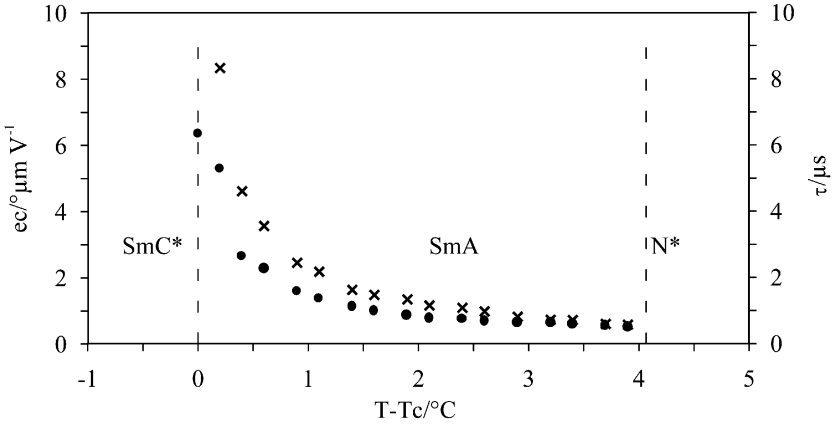

Figure 8. Relaxation time τ_S (●) of the soft mode and electroclinic coefficient e_C (**x**) in the SmA phase versus temperature for C12.

specially emphasized because of the proximity of the N*–SmA–SmC* multicritical point. The same relaxation mode has been observed in both, SmA and N* phases, for the C11 derivative [11]. Nevertheless, the relaxation frequencies of these modes (soft-mode in the SmA phase and relaxation process in the N* phase) have been located at 100 and 180 kHz, respectively in the SmA and N* phases. The transition from SmA to N* was picked out by changes of the df_s/dT slopes: $df_s/dT \approx 35$ and 320 kHz °C^{-1} in the SmA and N* phases, respectively. The relaxation process observed in the N* phase for the C11 compound persists only in 0.3°C above the SmA–N* transition temperature, whereas the temperature range of N* phase is about 8°C. Furthermore, the amplitude of this relaxation process was swiftly decreased and roughly vanished over 0.3°C. Unlike C10 and C11, we have not detected any relaxation process in the N* phase for C12 compound. Obviously, this continuous decrease of the amplitude of the relaxation mechanism in the N* phase, when passing from C10 to C11 compound and its disappearance for C12, is certainly connected with the proximity of an N*–SmA–SmC* multicritical point, which is closely related to chain length. Indeed, for a longer chain homologue (C12), the temperature range of SmA phase increases, and thus the N*–SmA–SmC* multicritical point seems to be far at atmospheric pressure. This can be also seen in the pressure–temperature (P–T) phase diagram of C12 presented in figure 9. The pressure and temperature ranges of SmC*, SmA, N* and I phases are identified from the phase sequence at atmospheric pressure. The phase transitions are reported in figure 9 as full lines for equlibrium curves (first order transitions); dashed lines give second order or very weak first order transitions. The (P–T) phase diagram clearly shows that the SmA and N* phases are stabilized upon application of pressure. The SmC*–SmA and SmA–N* transitions still then observed up to 300 bar and, consequently, the SmC*–SmA–N* multicritical point could be located at higher pressure, far from the atmospheric pressure condition. In fact, because of the vicinity of this point, the smectic fluctuations are favoured thermodynamically and are more or less important in the N* phase for C10 and C11, whereas for C12 the thermodynamic conditions are not favorable to induce these multicritical fluctuations. This probably explains the absence of the relaxation process attributed to local smectic order in N* phase of the C12 material.

5. Conclusion

Structural, thermodynamic, electrooptical and dielectric studies of a ferroelectric liquid crystal exhibiting the N*–SmA–SmC* phase sequence have been carried out as a function of temperature. From dielectric measurements, with and without bias voltage, we have studied the soft mode in the both SmA and SmC* phases. Using the experimental data without bias voltage, we have estimated the soft mode rotational viscosity and the free-energy coefficient. We have also determined a high value of the electroclinic effect in the SmA phase near the SmC*–SmA and SmA–N* phase transitions. The obtained experimental values of the electroclinic coefficient are much larger, and its amplitude was found to be connected to the polarization value in the SmC* phase via the piezoelectric coupling term. The main experimental result is that the relaxation mechanism detected at high frequencies in the N* phase for the compounds of the same series with shorter alkyloxy chains, is desapeared for the C12 homologue undertaking in this paper.

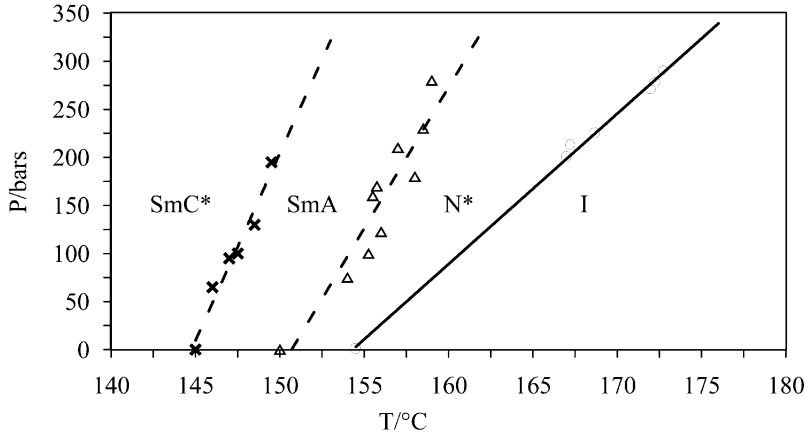

Figure 9. Pressure–temperature phase diagram of C12. Symbols denote the following transitions: (**x**) SmC*–SmA; (△) SmA–N* and (○) N*–I.

References

[1] S. Garoff, R.B. Meyer. *Phys. Rev. Lett.*, **38**, 848 (1977).
[2] G. Andersson, I. Dahl, P. Keller, W. Kuczynski, S.T. Lagerwall, K. Skarp, B. Stebler. *Appl. Phys. Lett.*, **51**, 640 (1987).
[3] C. Legrand, N. Isaert, J. Hmine, J.M. Buisine, J.P. Parneix, H.T. Nguyen, C. Destrade. *J. Phys., Paris, II*, **2**, 1545 (1992).
[4] H.T. Nguyen, A. Babeau, C. Léon, J.P. Marcerou, C. Destrade, A. Soldera, D. Guillon, A. Skoulios. *Liq. Cryst.*, **9**, 253 (1992).
[5] M. Marzec, R. Dabrowski, A. Fafara, W. Haase, S. Hiller, S. Wrobel. *Ferroelectrics*, **180**, 127 (1996).
[6] L. Komitov, S.T. Lagerwall, B. Stebler, G. Andersson, K. Flatischler. *Ferroelectrics*, **114**, 167 (1991).
[7] S.D. Lee, J.S. Patel. *Phys. Rev. Lett. A*, **155**, 435 (1991).
[8] C. Legrand, N. Isaert, J. Hmine, J.M. Buisine, J.P. Parneix, H.T. Nguyen, C. Destrade. Ferroelectrics, **121**, 21 (1991).
[9] A.M. Biradar, S.S. Bawa, K. Saxena, S. Chandra. *J. Phys., Paris, II*, **3**, 1787 (1993).
[10] J.P. Marcerou. *J. Phys., Paris, II*, **4**, 751 (1994).
[11] J. Hmine, C. Legrand, N. Isaert, H.T. Nguyen. *Liq. Cryst.*, **30**, 227 (2003).
[12] F. Grandjean. *C. r. hebd. Séance Acad. Sci., Paris*, **172**, 71 (1922).
[13] R. Cano. *Bull. Soc. Fr. Min. Cryst.*, **91**, 20 (1968).
[14] N.A. Clark, S.T. Lagerwall. *Appl. Phys. Lett.*, **36**, 899 (1980).
[15] J.M. Buisine, B. Soulestin, J. Billard. *Mol. Cryst. liq. Cryst.*, **91**, 115 (1983); J.M. Buisine, B. Soulestin, J. Billard. *Mol. Cryst. liq. Cryst.*, **97**, 397 (1983); J.M. Buisine. *Mol. Cryst. liq. Cryst.*, **109**, 143 (1983).
[16] C. Legrand, J.P. Parneix. *J. Phys., Paris*, **51**, 787 (1990).
[17] M. Brunet, N. Isaert. Ferroelectrics, **84**, 25 (1988).
[18] T. Carlsson, B. Zeks, A. Levstik, C. Filipic, I. Levstik, R. Blinc. *Phys. Rev. A*, **42**, 877 (1990).
[19] S.M. Khened, S. Krishna Prasad, B. Shivkuma, B.K. Sodashiva. *J. Phys., Paris*, **2**, 171 (1991).
[20] L.M. Blinov, L.A. Beresnev, W. Haase. *Ferroelectrics*, **181**, 211 (1996).
[21] Z. Li, G.A. Di Lisi, R.G. Petschek, C. Rosenblatt. *Phys. Rev. A*, **41**, 1997 (1990).
[22] C.H. Bahr, G. Heppke. *Liq. Cryst.*, **2**, 285 (1987).